

# Lawrence Berkeley National Laboratory

## Lawrence Berkeley National Laboratory

### **Title**

Ferrimagnetic ordering of single crystal Fe<sub>1-x</sub>Gax thin films

### **Permalink**

<https://escholarship.org/uc/item/5qq5t7cd>

### **Author**

McClure, A.

### **Publication Date**

2010-06-29

Peer reviewed

# Ferrimagnetic ordering of single crystal $\text{Fe}_{1-x}\text{Ga}_x$ thin films

Adam McClure<sup>a)</sup>

*Department of Physics, Montana State University, Bozeman, Montana 59715*

E. Arenholz

*Advanced Light Source, Lawrence Berkeley National Laboratory, Berkeley, California 94720*

Y. U. Idzerda

*Department of Physics, Montana State University, Bozeman, Montana 59715*

(Received 16 October 2009; accepted 17 May 2010; published 29 June 2010)

Molecular beam epitaxy was used to deposit body centered cubic single crystal  $\text{Fe}_{1-x}\text{Ga}_x$  thin films on  $\text{MgO}(001)$  and  $\text{ZnSe}/\text{GaAs}(001)$  substrates well beyond the bulk stability concentration of about 28%. The crystal quality of the substrate surface and each deposited layer was monitored *in situ* by reflection high energy electron diffraction. The magnetization of the samples as a function of Ga is found to decrease more rapidly than a simple dilution effect, and element-specific x-ray magnetic circular dichroism ascribes this trend to a decrease in the Fe moment and an induced moment in the Ga that is antialigned to the Fe moment.

## I. INTRODUCTION

Alloys of  $\text{Fe}_{1-x}\text{Ga}_x$  have generated recent interest because of their unique magnetostrictive and high tensile loading properties<sup>1-4</sup> and as possible spin polarized current injectors into GaAs-based light emitting diodes.<sup>5</sup> Of particular interest is the anisotropic behavior of the elastic constants as a function of Ga concentration, where  $\lambda_{100}$  is observed to increase tenfold while  $\lambda_{111}$  remains small and changes sign.<sup>3</sup> Furthermore, at the appropriate alloy concentrations, these materials have the ability to induce large magnetostriction with a small applied magnetic field.<sup>4</sup> Pinning a highly magnetostrictive material to a substrate and applying a magnetic field will impart an anisotropic stress, controllable by the magnetic field, in the  $\text{Fe}_{1-x}\text{Ga}_x$  film that may modify other magnetic properties of the film including magnetic anisotropy and magnetization dynamics, particularly the rate of precessional energy loss (damping).

## II. EXPERIMENT

Single crystal thin films ( $\sim 17$  nm) of  $\text{Fe}_{1-x}\text{Ga}_x$  ( $0 < x < 0.60$ ) were deposited on  $\text{MgO}(001)$  and  $\text{ZnSe}(80 \text{ nm})/\text{GaAs}(001)$  substrates by molecular beam epitaxy (MBE). Details of the  $\text{Fe}_{1-x}\text{Ga}_x$  growth on the epitaxial ZnSe buffer layer have been previously reported.<sup>6</sup> The polished MgO surface was prepared by first sonicating in acetone for 5 min, then rinsing in methanol, and followed by drying with flowing nitrogen. The typical third step in the triple clean process, the rinsing in de-ionized water, was skipped due to the hygroscopic nature of the substrate. The last step in the cleaning process was to heat the substrates to  $800^\circ\text{C}$  for 2 min in ultrahigh vacuum conditions to remove any other surface contaminants, as this treatment promotes layer-by-layer growth.<sup>7</sup>

The 17 nm epitaxial  $\text{Fe}_{1-x}\text{Ga}_x$  thin films were deposited at a rate of  $1.9 \text{ \AA}/\text{min}$  from independent Fe and Ga Knudsen cell sources at a substrate temperature of  $150^\circ\text{C}$ . The samples were capped with  $40 \text{ \AA}$  of Al to protect the  $\text{Fe}_{1-x}\text{Ga}_x$  films from the formation of any oxides. The Al layer was deposited at a substrate temperature of  $100^\circ\text{C}$  and a deposition rate of  $3.5 \text{ \AA}/\text{min}$ . Film thicknesses and compositions were determined by Rutherford backscattering (RBS) and x-ray absorption spectroscopy (XAS). RBS spectra were collected at multiple angles to eliminate the effects of channeling.

## III. RESULTS AND DISCUSSION

The crystal quality of the MgO surface and each deposited layer was monitored *in situ* by reflection high energy electron diffraction (RHEED) using 10 keV electrons. Representative RHEED patterns of the  $\text{MgO}(001)$  substrates and the  $\text{Fe}_{1-x}\text{Ga}_x(001)$  depositions are shown in Fig. 1. The sharp and continuous streaks seen for the  $\text{FeGa}(001)$  layer indicate a bcc growth of high crystal quality. RHEED of the  $\text{MgO}(001)$  substrate shows a clean, single crystal surface; however, the insulating nature of MgO makes obtaining a sharp RHEED pattern difficult, and the MgO RHEED images shown in Fig. 1 have been digitally modified. The RHEED patterns and subsequent vibrating sample magnetometry (VSM) measurements confirm the epitaxial relationship of  $\langle 110 \rangle \text{FeGa}(001) \parallel \langle 100 \rangle \text{MgO}(001)$ ,<sup>8,9</sup> and reveal a thin film crystal stability limit of about 45% Ga, higher than the bulk but less than growths on  $\text{ZnSe}/\text{GaAs}(001)$ .<sup>6</sup> Above that Ga concentration, the RHEED patterns become increasingly complex, while the hysteresis loops display multiphase behavior.

The substrate temperature of  $150^\circ\text{C}$  was chosen to optimize the crystal quality of the samples. Interestingly, RHEED images of pure Fe deposited on  $\text{MgO}(001)$  for a range of substrate temperatures look similar to those dis-

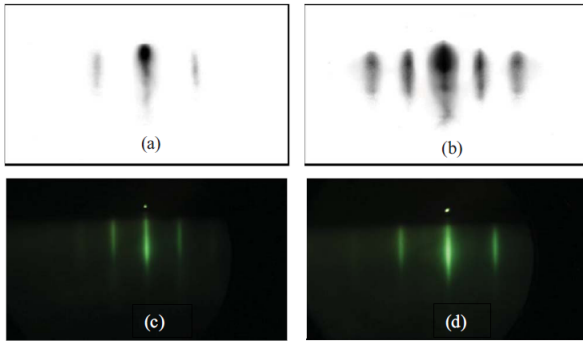


FIG. 1. (Color online) RHEED patterns recorded at an electron energy of 10 keV with the electron beam incident along the  $\langle 100 \rangle$  and  $\langle 110 \rangle$  crystallographic directions, respectively, of the bare MgO(001) substrate [(a) and (b)] and the 17 nm  $\text{Fe}_{0.82}\text{Ga}_{0.18}$  film [(c) and (d)]. The MgO RHEED images have been digitally modified to enhance the contrast.

played in Fig. 1, indicating quality single crystal *surfaces*; however, the internal structure of the films, probed by measuring the magnetic hysteresis of the samples, depends strongly on the deposition temperatures. As can be seen in Fig. 2(a), magnetic hysteresis loops taken along the hard axis ( $\langle 110 \rangle$ ) of the Fe films show much improved magnetic properties for the films deposited at a substrate temperature below 200 °C. Figure 2(b) shows hysteresis loops taken along the easy axis ( $\langle 100 \rangle$ ) of the Fe films deposited at 90 and 150 °C, and establishes 150 °C as the preferred deposition temperature due to the much reduced coercivity. A similar improvement in coercivity is measured for the hard axis.

Magnetometry measurements can also be used to monitor the magnetic anisotropy of these films as a function of Ga concentration. Figure 3 shows the in-plane magnetic hysteresis loops taken on 17 nm (a)  $\text{Fe}_{0.85}\text{Ga}_{0.15}$ (001) and (b)  $\text{Fe}_{0.735}\text{Ga}_{0.265}$ (001) samples and highlights two fundamental magnetic properties of  $\text{Fe}_{1-x}\text{Ga}_x$  thin films deposited on MgO(001): the purely cubic nature of the magnetic anisotropy, in contrast to an additional Ga dependent in-plane uniaxial anisotropy term for  $\text{Fe}_{1-x}\text{Ga}_x$  thin films deposited on ZnSe(80 nm)/GaAs(001) substrates,<sup>6</sup> and the change in sign

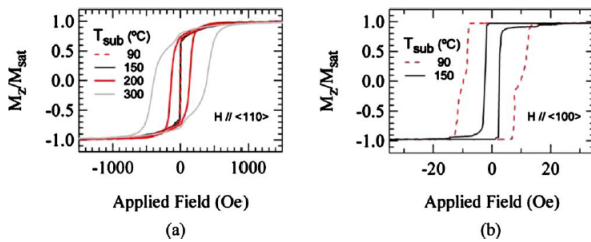


FIG. 2. (Color online) (a) Normalized magnetic hysteresis loops for 17 nm thin film Fe samples deposited on MgO(001) substrates for various substrate temperatures with the magnetic field applied along  $\langle 110 \rangle$ . (b) Normalized hysteresis loops measured along Fe(100) for substrate deposition temperatures of 90 °C and 150 °C.

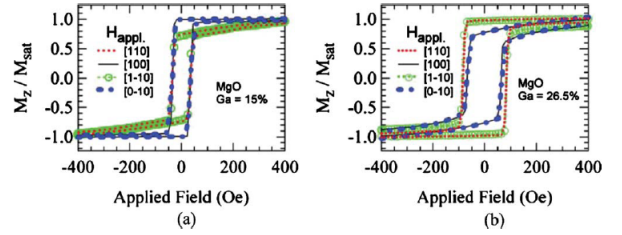


FIG. 3. (Color online) Normalized hysteresis loops taken along the indicated applied field directions for (a)  $\text{Fe}_{0.85}\text{Ga}_{0.15}$  and (b)  $\text{Fe}_{0.735}\text{Ga}_{0.265}$  thin films. Note the change in easy axis from  $\langle 100 \rangle$  for  $x=0.15$  (a) to  $\langle 110 \rangle$  for  $x=0.265$  (b) as well as the cubic symmetry.

of the cubic magnetic anisotropy constant  $K_1$ , indicated by the exchange of the easy and hard axes as the Ga concentration is increased.

Although there is a difference in the behavior of the magnetic anisotropy and the limits of stability for  $\text{Fe}_{1-x}\text{Ga}_x$  films deposited on MgO(001) and ZnSe/GaAs(001) substrates, the behavior of the magnetization and electronic structure are found to be independent of the underlying substrate. Vibrating sample magnetometry and RBS were used to determine the magnetizations of our films. The magnetizations for films grown on MgO(001) and ZnSe/GaAs(001) display an identical linear reduction with increasing Ga concentration up to about 23% Ga, and then decreasing more rapidly at higher concentrations. The initial decline in the magnetization is

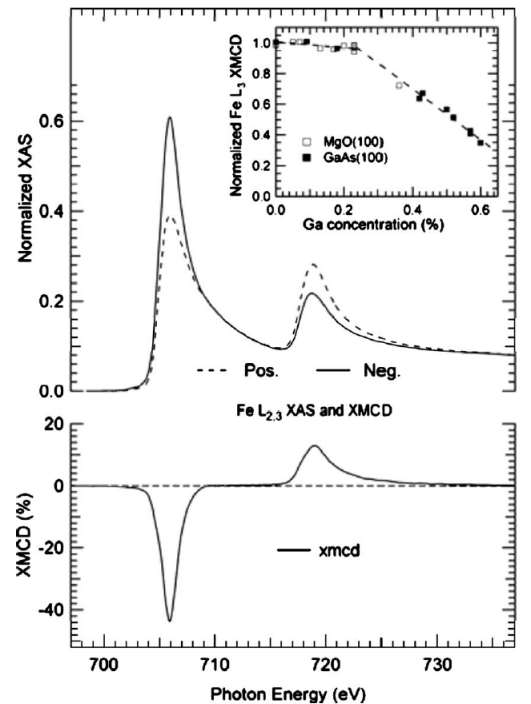


FIG. 4. Normalized Fe  $L_{2,3}$  edge XAS and XMCD for  $\text{Fe}_{0.80}\text{Ga}_{0.20}$  film at room temperature. Inset: The measured variation of the Fe  $L_3$  XMCD peak intensity as a function of Ga concentration. The dashed line is a guide to the eyes.

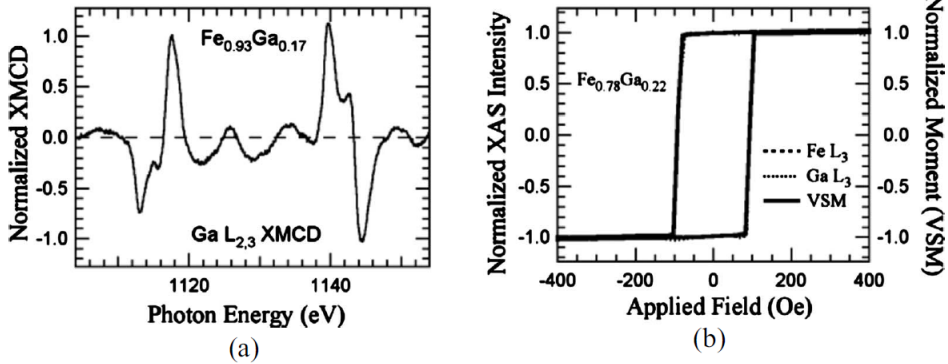


FIG. 5. (a) Ga  $L_{2,3}$  XMCD for 17 nm  $\text{Fe}_{0.83}\text{Ga}_{0.17}$  film. (b) Element specific magnetic hysteresis loops for Fe and Ga. Included is the total moment hysteresis loop as measured by VSM. The high degree of similarity between these loops shows that the Fe and Ga are strongly coupled and no secondary magnetic phase is present.

slightly reduced from the effect of adding a nonmagnetic element (Ga) to a magnetic host (Fe) of constant moment.

To further investigate the origin of the magnetization reduction, we performed x-ray magnetic circular dichroism (XMCD) at the Fe and Ga  $L_{2,3}$ -edges for growths on both substrates, acquired by sample current yield with the films magnetically saturated at beamline 4.0.2 of the Advanced Light Source at Lawrence Berkeley National Laboratory. XMCD is an element-specific technique using circular polarized photons and measuring the differential XAS between having the photon helicity and sample magnetization aligned and antialigned. The peak intensity of the XMCD signal is proportional to the elemental magnetic moment.<sup>10-12</sup>

Figure 4 shows the aligned and antialigned Fe  $L_{2,3}$  XAS of an  $\text{Fe}_{0.80}\text{Ga}_{0.20}$  sample and the resultant dichroism spectra, taken at fixed photon helicity and reversing the magnetization of the sample at each photon energy. The inset tracks the Fe  $L_3$  peak XMCD intensity as a function of Ga concentration, showing that the Fe XMCD decreases gradually out to about 23% Ga, where the Fe moment is still about 95% that of pure Fe, and where the Fe XMCD intensity decreases more precipitously.

The trend of the Fe XMCD as a function of Ga resembles that of the magnetization and does enhance the magnetization reduction. Additional information concerning the magnetization reduction can be found in the Ga moment behavior. Therefore, we performed XMCD measurements at the Ga  $L_{2,3}$  edges for each film. By comparing to theoretical electronic structure calculations for FeGa alloys<sup>13,14</sup> and other experimental Ga spectra for Mn-doped GaAs,<sup>15</sup> we conclude that the presence and sign of the signal, as shown in Fig. 5(a) for  $\text{Fe}_{0.83}\text{Ga}_{0.17}$ , establish an induced local moment in the Ga that is aligned antiparallel to the Fe moment,<sup>13-15</sup> in agreement with the theoretical calculations.

One remaining concern is that the Ga may have segregated into a secondary magnetic phase independent of the majority of the Fe. To eliminate this possibility, element-specific magnetic hysteresis (MHY) loops of the Fe and Ga were separately acquired for the films. Element specific MHY loops are x-ray absorption intensities collected using

fixed helicity circularly polarized light, at the photon energy corresponding to the peak  $L_3$  XMCD intensity, while sweeping the magnetic field.<sup>16,17</sup> Figure 5(b) shows normalized MHY loops for Fe and Ga in an  $\text{Fe}_{0.78}\text{Ga}_{0.22}$  film, along with the total moment VSM hysteresis data collected on the same sample. In all instances, the field was applied along the  $\langle 110 \rangle$  easy axis of the sample, and the results demonstrate that the Fe and Ga moments are inherently linked.

#### IV. SUMMARY

MBE was used to deposit single crystal  $\text{Fe}_{1-x}\text{Ga}_x$  thin films on MgO(001) substrates up to 45% Ga concentration. These depositions show purely cubic magnetic anisotropy, in contrast to an additional Ga dependent in-plane uniaxial anisotropy for  $\text{Fe}_{1-x}\text{Ga}_x$  thin films deposited on ZnSe(80 nm)/GaAs(001) substrates, though a similar change in sign of the cubic magnetic anisotropy constant,  $K_1$ , is seen for both sets of samples. The decrease in the magnetization with the incorporation of Ga also shows a similar trend for the depositions on both substrates and has been attributed to a decrease in the Fe moment along with an induced moment in the Ga that is antialigned to the Fe moment.

#### ACKNOWLEDGMENTS

This research was supported by the Army Research Office under Grant No. W911NF-08-1-0325. The Advanced Light Source is supported by the Director, Office of Science, Office of Basic Energy Sciences, of the U.S. Department of Energy under Contract No. DE-AC02-05CH11231.

<sup>1</sup>A. E. Clark, J. B. Restorff, M. Wun-Fogle, T. A. Lograsso, and D. L. Schlagel, IEEE Trans. Magn. **36**, 3238 (2000).

<sup>2</sup>A. E. Clark, M. Wun-Fogle, J. B. Restorff, T. A. Lograsso, and J. R. Cullen, IEEE Trans. Magn. **37**, 2678 (2001).

<sup>3</sup>A. E. Clark, K. B. Hathaway, M. Wun-Fogle, J. B. Restorff, T. A. Lograsso, V. M. Keppens, G. Petculescu, and R. A. Taylor, J. Appl. Phys. **93**, 8621 (2003).

<sup>4</sup>R. A. Kellogg, A. B. Flatau, A. E. Clark, M. Wun-Fogle, and T. Lograsso, J. Intell. Mater. Syst. Struct. **16**, 471 (2005).

<sup>5</sup>O. M. J. van 't Erve, C. H. Li, G. Kioseoglou, A. T. Hanbicki, M. Osofsky, S.-F. Cheng, and B. T. Jonker, Appl. Phys. Lett. **91**, 122515

- (2007).
- <sup>6</sup>A. McClure, S. Albert, T. Jaeger, H. Li, P. Rugheimer, J. A. Schaefer, and Y. U. Idzerda, *J. Appl. Phys.* **105**, 07A938 (2009).
- <sup>7</sup>T. Koyano, E. Kita, K. Ohshima, and A. Tasaki, *J. Phys.: Condens. Matter* **3**, 5921 (1991).
- <sup>8</sup>T. Kanaji, K. Asano, and S. Nagata, *Vacuum* **23**, 55 (1973).
- <sup>9</sup>J. F. Bobo *et al.*, *Eur. Phys. J. B* **24**, 43 (2001).
- <sup>10</sup>B. T. Thole, P. Carra, F. Sette, and G. van der Laan, *Phys. Rev. Lett.* **68**, 1943 (1992).
- <sup>11</sup>P. Carra, B. T. Thole, M. Altarelli, and X. Wang, *Phys. Rev. Lett.* **70**, 694 (1993).
- <sup>12</sup>C. T. Chen, Y. U. Idzerda, H.-J. Lin, N. V. Smith, G. Meigs, E. Chaban, G. H. Ho, E. Pellegrin, and F. Sette, *Phys. Rev. Lett.* **75**, 152 (1995).
- <sup>13</sup>R. Wu, *J. Appl. Phys.* **91**, 7358 (2002).
- <sup>14</sup>J. M. Hill, R. J. McQueeney, R. Wu, K. Dennis, R. W. McCallum, M. Huang, and T. A. Lograsso, *Phys. Rev. B* **77**, 014430 (2008).
- <sup>15</sup>D. J. Keavney, D. Wu, J. W. Freeland, E. Johnston-Halperin, D. D. Awschalom, and J. Shi, *Phys. Rev. Lett.* **91**, 187203 (2003).
- <sup>16</sup>C. T. Chen, Y. U. Idzerda, H.-J. Lin, G. Meigs, A. Chaaiken, G. A. Prinz, and G. H. Ho, *Phys. Rev. B* **48**, 642 (1993).
- <sup>17</sup>V. Chakarian, Y. U. Idzerda, G. Meigs, E. E. Chaban, J.-H. Park, and C. T. Chen, *Appl. Phys. Lett.* **66**, 3368 (1995).